Self-incompatibility response induced by calcium increase in sperm of the ascidian *Ciona intestinalis*

Takako Saito[a], Kogiku Shiba[b], Kazuo Inaba[b], Lixy Yamada[a,1], and Hitoshi Sawada[a,1]

[a]Sugashima Marine Biological Laboratory, Graduate School of Science, Nagoya University, Toba, Mie 517-0004, Japan; and [b]Shimoda Marine Research Center, University of Tsukuba, Shimoda, Shizuoka 415-0025, Japan

Edited by Ryuzo Yanagimachi, Institute for Biogenesis Research, University of Hawaii, Honolulu, HI, and approved February 1, 2012 (received for review September 19, 2011)

Many hermaphroditic organisms possess a self-incompatibility system to avoid self-fertilization. Recently, we identified the genes responsible for self-sterility in a hermaphroditic primitive chordate (ascidian), *Ciona intestinalis*: sperm-side polycystin 1-like receptors *s-Themis-A/B* and egg-side fibrinogen-like ligands on the vitelline coat (VC) *v-Themis-A/B*. Here, we investigated the sperm behavior and intracellular Ca^{2+} concentration ($[Ca^{2+}]_i$) in response to self/nonself-recognition. We found that sperm motility markedly decreased within 5 min after attachment to the VC of self-eggs but not after attachment to the VC of nonself-eggs and that the apparent decrease in sperm motility was suppressed in low Ca^{2+} seawater. High-speed video analysis revealed that sperm detached from the self-VC or stopped motility within 5 min after binding to the self-VC. Because s-Themis-B contains a cation channel domain in its C terminus, we monitored sperm $[Ca^{2+}]_i$ by real-time $[Ca^{2+}]_i$ imaging using Fluo-8H-AM (AAT Bioquest, Inc.). Interestingly, we found that sperm $[Ca^{2+}]_i$ rapidly and dramatically increased and was maintained at a high level in the head and flagellar regions when sperm interacted with the self-VC but not when the sperm interacted with the nonself-VC. The increase in $[Ca^{2+}]_i$ was also suppressed by low-Ca^{2+} seawater. These results indicate that the sperm self-recognition signal triggers $[Ca^{2+}]_i$ increase and/or Ca^{2+} influx, which elicits a self-incompatibility response to reject self-fertilization in *C. intestinalis*.

Sexual reproduction is an essential process to elicit genetic diversity in the next generation. Therefore, many hermaphrodite species have acquired a self-incompatibility (SI) system that prevents inbreeding. In flowering plants, SI systems depend on S proteins, which are encoded in an SI specificity-determining locus (1). The invertebrate chordate *Ciona intestinalis* is a hermaphroditic animal that releases sperm and eggs nearly simultaneously and exhibits strict self-sterility. These features were reported by Tomas Hunt Morgan about a century ago (2). Rosati and De Santis (3) and Kawamura et al. (4) later clarified that a self/nonself-discrimination site resides on the vitelline coat (VC), an acellular matrix surrounding the egg, and that the VC shows higher affinity to allogeneic (nonself) sperm than to autologous (self) sperm (3, 4). Recently, we revealed that the SI system in *C. intestinalis* is controlled by two multiallelic independent loci, loci A and B. Each of the loci contains a pair of SI candidate genes, egg-side *v-Themis-A/B* and sperm-side *s-Themis-A/B*. All four proteins show high polymorphisms among individuals. Comprehensive proteome analysis of the isolated VC revealed that both v-Themis-A and v-Themis-B exist in the VC (5, 6). Interestingly, *v-Themis-A/B* genes reside in the cDNA strand of the first intron of *s-Themis-A/B* genes, respectively, suggesting that these egg- and sperm-side SI factors would be hardly segregated by homologous recombination during meiosis (5).

Although the basic mechanism of the SI system in *C. intestinalis* has been revealed, the allorecognition-induced sperm behavior and the intracellular signals are still unknown. In the present study, therefore, we investigated the motility and behavior of sperm by high-speed video microscopy after sperm interaction with the VC of self- and nonself-eggs. We also analyzed the intracellular Ca^{2+} concentration ($[Ca^{2+}]_i$) by a Ca^{2+} imaging technique using a fluorescent Ca^{2+} indicator under a fluorescent microscope before and after the adhesion of sperm to the VC isolated from self- and nonself-eggs.

Results and Discussion

Sperm Motility and Behavior During Binding to the Self-VC and Nonself-VC. We first investigated the motility of sperm attached to the egg VC using eggs treated with glycerol to reveal the difference between self- and nonself-insemination. Glycerinated eggs are useful for evaluating the sperm binding process, because these eggs are metabolically inert and also because sperm undergo neither the acrosome reaction nor penetration through the VC (3). Because glycerinated eggs were rotated and moved by active sperm attached to the VC, the difference between self-binding and nonself-binding was monitored by measuring the distance that glycerinated eggs moved in 1 s (Fig. 1*A*). Results obtained in artificial seawater (ASW) showed that sperm are able to maintain their binding to the VC of nonself-eggs at a constant movement for at least 5 min after insemination [Fig. 1*B* and Movie S1 *A* (nonself, 1 min) and *C* (nonself, 5 min)]. On the other hand, the distances that glycerinated eggs moved in 1 s at 1 min after self-insemination appeared to be slightly less than the distances that the eggs moved after nonself-insemination [Fig. 1*B* and comparison between Movie S1 *A* (nonself, 1 min) and *B* (self, 1 min)]. Furthermore, almost no rotation or movement of the eggs was observed at 5 min after self-insemination [Fig. 1*B* and Movie S1*D* (self, 5 min)]. These results indicate that self-sperm cause an SI response during a period of 5 min after insemination.

We then analyzed the behavior of sperm after attachment to the VC and also the flagellar beating under a phase-contrast microscope equipped with a power light-emitting diode (LED) stroboscopic illumination system (7). To compare the interactions between sperm and eggs directly, sperm were added to a suspension of glycerinated self- and nonself-eggs, which were placed closely, and the autologous and allogeneic sperm-egg interactions were directly compared under the same conditions in the same view by microscopy (Fig. 2*A* and Movie S2 *A* and *B*). As shown in Movie S2 *A* and *B*, the number of bound sperm and sperm motility on the self-VC at 5 min after insemination were considerably less than those on the nonself-VC, although no prominent difference was observed at 1 min after insemination. We then quantitatively compared the sperm binding to these VCs by counting the bound sperm under a microscope. It was

Author contributions: T.S., L.Y., and H.S. designed research; T.S. and K.S. performed research; K.S. and K.I. contributed new reagents/analytic tools; T.S., K.S., K.I., L.Y., and H.S. analyzed data; and T.S., L.Y., and H.S. wrote the paper.

The authors declare no conflict of interest.

This article is a PNAS Direct Submission.

[1]To whom correspondence may be addressed. E-mail: lyamada@bio.nagoya-u.ac.jp or hsawada@bio.nagoya-u.ac.jp.

This article contains supporting information online at www.pnas.org/lookup/suppl/doi:10.1073/pnas.1115086109/-/DCSupplemental.

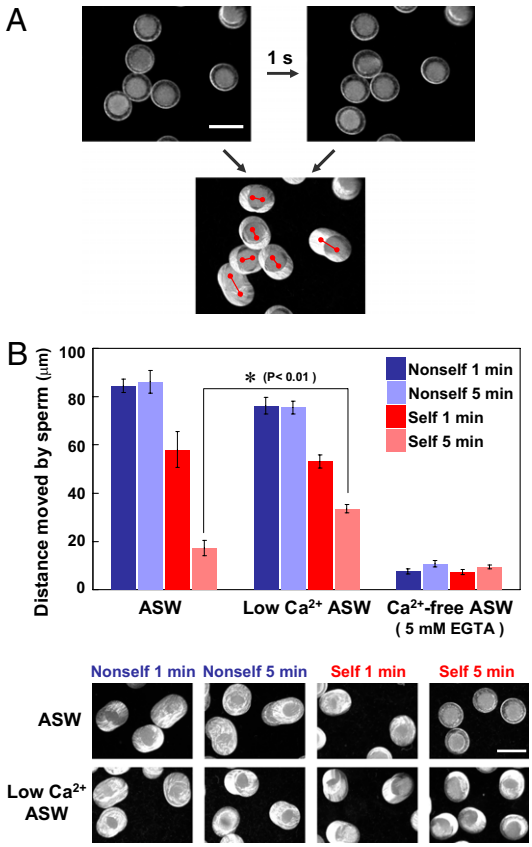

Fig. 1. Sperm motility monitored by rotation and movement of glycerinated eggs. (*A*) Moving distances from the starting points (*Left*) to the ending points (*Right*) during a period of 1 s after the addition of sperm to the glycerinated eggs were measured and used as criteria of sperm binding and movement. (Scale bar, 200 μm.) (*B*) Moved distances of glycerinated eggs by sperm during a period of 1 s in ASW, Ca^{2+}-free ASW (low-Ca^{2+} ASW), and Ca^{2+}-free ASW containing 5 mM EGTA were measured. The bars represent means ± SEM (n = 30). (Scale bar, 200 μm.) *P < 0.01 (Student t test).

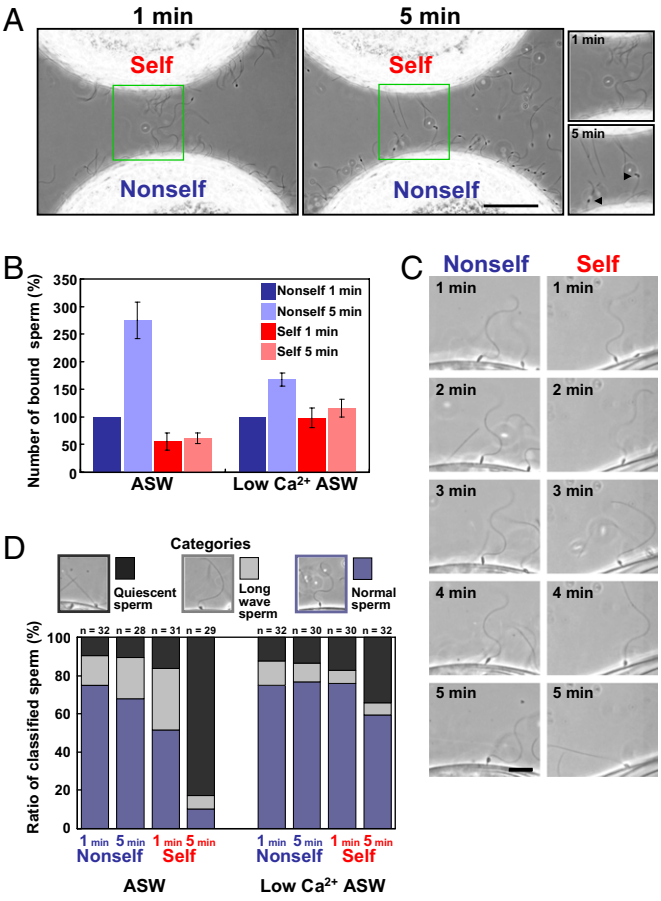

Fig. 2. Sperm behavior in self- and nonself-inseminations. (*A*) Appearances of sperm added to the self- and nonself-glycerinated eggs, both of which were put in the same view. Sperm motility and behavior are shown in the large panels (Movie S2) after 1 min (*Left*) and 5 min (*Right*). The small panels show enlarged views of the large panels. The arrowheads show mitochondria. (Scale bar, 50 μm.) (*B*) Binding of sperm to the eggs. The numbers of sperm bound to the self- and nonself-glycerinated eggs in the same focus were counted and expressed as the number of sperm per 100 μm of the VC. The increasing rate was normalized on the basis of the number of sperm bound to the nonself-VC at 1 min after insemination in ASW and low-Ca^{2+} ASW. The bars represent means ± SEM (n = 4). (*C*) Example of the waveform observed from 1 to 5 min after insemination. In nonself-insemination, sperm-moving behaviors at 5 min after insemination appear to be the same as those at 1 min after insemination. In contrast, sperm showed a drastic change in waveform and became quiescent in the case of self-insemination at 5 min. (Scale bar, 10 μm.) (*D*) Ratio of sperm classified into three categories on the basis of curvature of their flagella morphology: regularly waving sperm (normal sperm), asymmetrically bending sperm with the increased wavelength (long-wave sperm), and quiescent sperm. The number of counted sperm is indicated in each column.

found that the number of bound sperm on the nonself-VC was larger than that on the self-VC even at 1 min after insemination (Fig. 2*B*). Furthermore, the number of bound sperm on the nonself-VC gradually increased during a period of 5 min, whereas there was no significant increase in the case of self-insemination (Fig. 2 *A* and *B* and Movie S2 *A* and *B*). These apparent differences caused a marked difference in the binding ability toward the self-VC and nonself-VC at 5 min after insemination. These results clearly show that self-sperm triggers an SI response within 5 min after insemination.

During the course of this study, we noticed that sperm that had attached to the VC of nonself-eggs, but not sperm that had attached to the VC of self-eggs, underwent mitochondrial swelling, migration, and shedding, designated "sperm reaction" (8, 9). These observations imply that the sperm reaction is blocked when sperm recognized the VC as self. Alternatively, the sperm reaction may be actively induced when sperm recognized the VC as nonself.

Close inspection by live imaging experiments revealed that the waveform of most sperm flagella suddenly changed to an asymmetrical pattern with largely increased wavelength, resulting in a quiescent state after the attachment of sperm to the self-egg VC (Fig. 2*C*). This waveform change was observed in all sperm at the moment of the sperm binding to the VC as a result of the collision of sperm with the VC. However, sperm recovered their regular beating after the asymmetrical pattern in the case of nonself-insemination. On the other hand, the waveform and motility of most of the sperm on the VC of self-eggs changed again during a period of 5 min: In a representative case, the waveform of flagella appeared normal within 2 min but gradually changed to the asymmetrical pattern at about 3 min and became quiescent at 5 min (Fig. 2*C*). Some other sperm detached from the self-VC instead of becoming quiescent (Fig. S1). Taking these phenomena into account, the reason why no apparent increase was observed in the number of sperm bound to the self-VC during the 5-min period (Fig. 2*B*) is considered to be attributable to sperm detachment from the VC.

To analyze these phenomena further, we classified sperm into three categories on the basis of flagellar curvature, and the

number of sperm in each category is summarized in Fig. 2*D*. Flagellar waveform in nonself-insemination showed little or no difference at 1 min and 5 min after insemination. In contrast, 80% of the sperm straightened their flagella and became quiescent at 5 min after self-insemination in ASW (Fig. 2*D*). These results indicate that sperm show an SI response within 5 min, including detachment from the VC and characteristic changes in flagellar movement in self-insemination. Thus, it is concluded that self-recognition causes the SI response, which triggers rejection signal(s) to self-fertilization.

Ca^{2+} Functions in the SI System. The sperm-side SI candidate genes *s-Themis-A/B* show homology to mammalian *PKD1*, and s-Themis-B possesses a cation channel domain in its C-terminal region (5) (Fig. S2). Although *s-Themis-A/B* shows such homology, it is known that *C. intestinalis* has both *PKD1* and *PKD2* orthologous genes that are distinct from *s-Themis-B*, a family of PKD transient receptor potential polycystic (TRPP)-related channel (10). Therefore, *s-Themis-A/B* appears to evolve independently from *PKD1* and *PKD2*. Mammalian *PKD1* encodes Polycystin-1 (PC1), which is associated with a TRP-type Ca^{2+}-permeable nonselective cation channel, named Polycystin-2 (PC2) (11, 12). A complex of PC1 and PC2 regulates the level of intracellular Ca^{2+} in the kidney (11, 13). It is known that PKD1 family members of other organisms play key roles in fertilization. Mouse PKDREJ, which contains a cation-channel domain in its C-terminal region, is located in the sperm head acrosomal region (14), and the sea urchin sperm homolog of PC2 (suPC2) colocalizes with the PC1 homolog REJ3 in the plasma membrane over the acrosomal vesicle (15). It has been proposed that the suPC2–REJ3 complex functions as a cation channel responsible for the acrosome reaction when sperm make contact with the jelly layer surrounding the egg during fertilization (15). Taking the structures and functions of PKD1 family proteins into account, it seems plausible that s-Themis-B regulates Ca^{2+} influx by making a complex with s-Themis-A during the self/nonself-recognition process. Ca^{2+} is well known to be an important factor involved in fertilization and regulation of flagellar beating. In addition, intracellular Ca^{2+} plays a key role in sperm activation and chemoattractant (16). It is also reported that sperm flagella show a highly asymmetrical waveform at Ca^{2+} burst, which is mediated by sperm activating and attracting factor (SAAF) in *C. intestinalis* (7). In sea urchin sperm, the bending patterns of sperm flagella appear to depend on their $[Ca^{2+}]_i$ levels (17, 18). These findings led us to investigate whether the sperm SI response induces a certain change in $[Ca^{2+}]_i$.

To address this issue, we first examined the effects of extracellular Ca^{2+} on the ability of sperm to rotate and move the glycerinated self-egg (Fig. 1*B*). The distance moved by sperm showed no marked difference in 1 min between ASW and low-Ca^{2+} ASW (5 μM Ca^{2+}) in both the self-insemination and nonself-insemination (Fig. 1*B*, compare the first and third columns between ASW and low-Ca^{2+} ASW). In contrast, the decrease in sperm motility on the basis of the egg-moving distance was significantly suppressed at 5 min after self-insemination in low-Ca^{2+} ASW (Fig. 1*B*). Because external Ca^{2+} is necessary for fertilization processes, including sperm motility, chemotaxis, and acrosome reaction (or sperm reaction), it is impossible to carry out self-fertilization experiments in the absence of Ca^{2+} in surrounding ASW. In fact, no appreciable sperm motility was monitored in Ca^{2+}-free ASW containing 5 mM EGTA (Fig. 1*B*, second and third columns). In addition to sperm motility, apparent binding ability of sperm to the self-VC was stimulated by lowering the external Ca^{2+} concentration: The number of bound sperm to the self-VC in low-Ca^{2+} ASW was higher than that in regular ASW both at 1 and 5 min after self-insemination (Fig. 2*B*). These results suggest that the SI responses, such as detachment of sperm from the VC and decrease in sperm motility, depend on the extracellular Ca^{2+} concentration. These

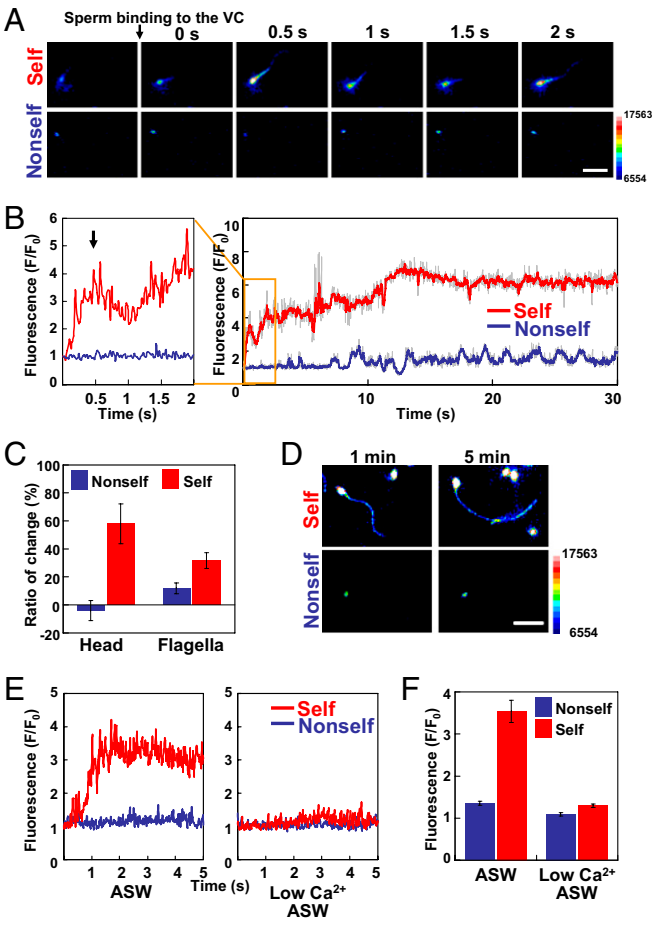

Fig. 3. $[Ca^{2+}]_i$ dynamics during the binding of sperm to self- and nonself-VCs. (*A*) $[Ca^{2+}]_i$ images of sperm before and after the binding of sperm to self- and nonself-VCs. Intervals between the images are 0.5 s. A color bar shows fluorescence intensity. (Scale bar, 10 μm.) (*B*) Relative fluorescent intensity attributable to $[Ca^{2+}]_i$ in the head region of a single sperm, which binds to the self-VC (red) and nonself-VC (blue), during a period of 30 s after the binding of sperm. $[Ca^{2+}]_i$ was expressed as F/F_0, which is a relative value of the fluorescence signals of the sperm head and flagella. F_0 means the fluorescence signals of swimming sperm before binding to the VC. An arrow indicates the first peak of $[Ca^{2+}]_i$. Fluorescence intensity was measured every 20 ms. Raw values of fluorescence are shown in gray, and the five-point simple moving average of raw values is shown in red or blue. (*C*) Increase in $[Ca^{2+}]_i$ in the sperm head and flagella regions in self- and nonself-inseminations. Relative fluorescence intensities in the head and flagella were expressed as the ratio (%) of the change in fluorescence from 1 min to 5 min after the binding of sperm to the nonself-VC (blue) and self-VC (red). The bars represent means ± SEM (n = 12, n = 16, n = 11, and n = 27 for nonself-head, self-head, nonself-flagella, and self-flagella, respectively). (*D*) Ca^{2+} fluorescence images of sperm at 1 and 5 min after insemination. A color bar indicates fluorescence intensity. (Scale bar, 10 μm.) (*E*) Relative fluorescent intensity attributable to $[Ca^{2+}]_i$ in the head region of a single sperm, which binds to the self-VC (red) and nonself-VC (blue), during a period of 5 s after the binding of sperm in ASW (*Left*) and low-Ca^{2+} ASW (*Right*). (*F*) Changes of relative fluorescent intensity in the sperm head under the conditions of ASW and low-Ca^{2+} ASW. F means the maximum value of the fluorescence signal of sperm, which bound to the VC, whereas F_0 means the value before the binding of sperm to the VC. The bars represent means ± SEM (n = 30).

results led us to investigate the possible involvement of intracellular Ca^{2+} in the self-signaling pathway.

$[Ca^{2+}]_i$ Increase Induced by the Self-Signal. To investigate precisely whether the self-signal induces change in $[Ca^{2+}]_i$, we carried out real-time Ca^{2+} imaging (7). Sperm were previously loaded with

a Ca^{2+} indicator dye, Fluo-8H-AM (AAT Bioquest, Inc.) and activated by SAAF (19–21). VCs isolated from self-eggs and nonself-eggs were placed on a slide glass and inseminated by the above sperm, and they were then observed under a fluorescence microscope. Interestingly, sperm underwent a rapid and marked increase in $[Ca^{2+}]_i$ both in the head and flagella within 30 s after the binding of sperm to the isolated self-VC (Fig. 3 *A* and *B* and Movie S3*A*). In contrast, such an increase in $[Ca^{2+}]_i$ was not observed in the sperm bound to the isolated nonself-VC (Fig. 3 *A* and *B* and Movie S3*A*). We also noticed that $[Ca^{2+}]_i$ in the sperm head transiently increased in 0.5 s (Fig. 3*B*, arrow) and then gradually increased again after binding to the self-VC (Fig. 3*B*). The level of $[Ca^{2+}]_i$ remained high for at least 5 min (Fig. 3 *C* and *D*). Although the increased levels of $[Ca^{2+}]_i$ in the head region were not constant among individuals, it was reproducibly observed that the sperm head $[Ca^{2+}]_i$ rapidly and transiently increased at about 0.5 s and then gradually increased again (Fig. 3*B*). No such increase in $[Ca^{2+}]_i$ was observed until 5 min in the sperm bound to the nonself-VC (Fig. 3 *C* and *D* and Movie S3*B*). $[Ca^{2+}]_i$ in sperm flagella also showed a pattern of increase in $[Ca^{2+}]_i$ similar to that in the sperm head region for at least 5 min (Fig. 3 *C* and *D*). We sometimes observed that sperm once bound to the self-VC detached from the self-VC (Movie S4). Although $[Ca^{2+}]_i$ increased in all sperm during the self-insemination, some of the sperm left the VC before completion of the increase in $[Ca^{2+}]_i$. To investigate whether the extracellular Ca^{2+} is necessary for the self-recognition–mediated increase in $[Ca^{2+}]_i$, we carried out the same Ca^{2+} imaging experiments in low-Ca^{2+} ASW. The results clearly showed that no significant increase in $[Ca^{2+}]_i$ was observed in the sperm head and tail regions during the binding of sperm to the self-VC under the conditions of low-Ca^{2+} ASW. These results suggest that the SI response is induced by Ca^{2+} influx-mediated $[Ca^{2+}]_i$ bursts in the sperm head and flagella, which appear to be capable of changing the sperm motility.

Because the activation of sperm motility is accompanied by an increase in intracellular pH (pH_i), the increase in fluorescence could be induced by the change in pH_i. Therefore, we measured the fluorescence of Ca^{2+}-bound Fluo-8H-AM in sperm after incubation with or without 5 μM nigericin, an H^+/K^+ ionophore, at pH 7.2, pH 7.6, and pH 8.2 in ASW to control the pH_i. Although the fluorescence of sperm appears to be influenced by extracellular pH, pH-dependent change in fluorescence was quite low (Fig. S3; within 25% difference) compared with the SI response, in which fluorescence of sperm after the binding to the self-VC was three- to sixfold higher than the value before the sperm binding (Fig. 3). These results indicate that the rapid and marked increase in fluorescence is certainly attributable to $[Ca^{2+}]_i$ within sperm.

In *C. intestinalis,* it has been reported that sperm $[Ca^{2+}]_i$ plays a key role in inducing the change in waveform of flagella in the chemotactic response of SAAF (7). Therefore, it seems plausible that $[Ca^{2+}]_i$ of sperm plays several roles in intracellular signaling during fertilization. However, the increased level of $[Ca^{2+}]_i$ in response to the self-signal appears to be extraordinarily high compared with the level in sperm chemotaxis. Thus, the level of $[Ca^{2+}]_i$ or the threshold may regulate several sperm responses. In connection with this, it is notable that $[Ca^{2+}]_i$ is an intracellular signal in pollen after its attachment to the surface of the self-stigma in the flowering plants of Papaveraceae (22). It is currently believed that the increase in $[Ca^{2+}]_i$ induces apoptosis via activation of caspase-like protease in Papaveraceae (22). By analogy, the rapid and marked increase in $[Ca^{2+}]_i$ in *C. intestinalis* sperm may induce sperm cell death, similar to the SI systems in Papaveraceae.

Flowering plants use distinct binding partners with high polymorphisms in the SI systems (1, 23, 24). In Brassicaceae, pollen *SP11/SCP* and stigma S-locus receptor kinase (*SRK*) genes are tightly linked in the same chromosome, making respective haplotypes; even in this family, an increase in intracellular Ca^{2+} in papilla cells in the stigma appears to play a key role in the SI system (1, 25). Taking into account these data, the SI system or the self/nonself-recognition system may be much more common between animals and plants than we have thought previously, even in the intracellular signaling pathway (26).

Further studies are necessary to elucidate the precise intracellular signaling networks leading to the rejection of self-fertilization. It also remains to be resolved whether s-Themis-B functions as a bona fide Ca^{2+} channel. However, if this is the case, PKD family proteins other than s-Themis might also function as a Ca^{2+} channel. Our present finding may shed light on the functional studies of PKD1 family proteins.

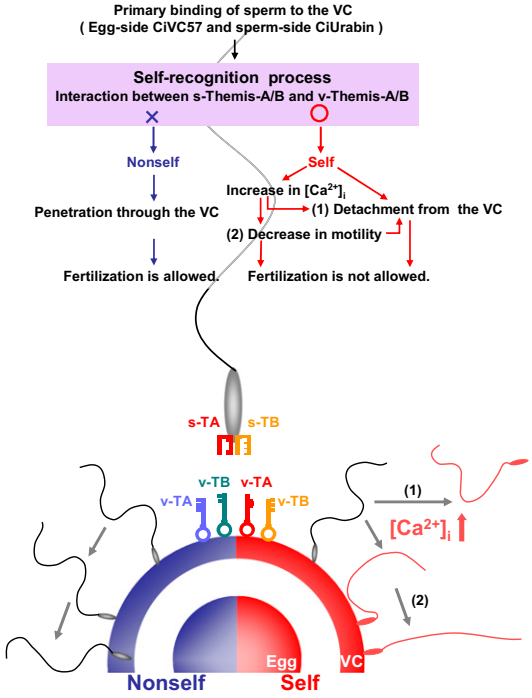

Fig. 4. Working hypothesis of the s/v-Themis–mediated SI system. We propose that sperm increase $[Ca^{2+}]_i$ and detach from the VC when both s-Themis-A/B (s-TA and S-TB; "keyholes") on the sperm surface recognize respective v-Themis-A/B (v-TA and v-TB; "keys") on the VC as self. Sperm remaining on the self-VC change their waveform and motility. On the other hand, nonself-sperm remain on the VC and penetrate through the VC to fertilize the egg (details are provided in the main text).

Conclusions

In the present report, we show that the self-recognition signal triggers Ca^{2+} influx in the sperm head and flagellar regions, which causes vigorous movement of the sperm followed by quiescence or by sperm detachment from the VC. It should be emphasized that this report shows intracellular signaling in the SI system in a hermaphroditic chordate.

Here, we propose a working hypothesis on the mechanism of the SI system in *C. intestinalis* (Fig. 4). Because s-Themis proteins recognize the autologous (or the same-haplotypic) v-Themis proteins rather than allogeneic ones, and also because the number of sperm that bound to the VC in nonself-insemination was significantly larger than that in self-insemination, certain gamete proteins other than s/v-Themis may play a key role in the primary binding process. Candidate proteins for the primary binding process are egg-side CiVC57 on the VC and sperm-side

CiUrabin, a GPI-anchored membrane protein, because these proteins are capable of interacting biochemically (27). After the primary binding, the self/nonself-recognition process must take place; however, when both s-Themis-A and s-Themis-B interact with v-Themis-A and v-Themis-B of the same haplotype, respectively, sperm must recognize the VC as self. In this case, sperm appear to allow the rapid influx of Ca^{2+}, which causes a drastic waveform change in sperm. As a result, some sperm may become quiescent and others may detach from the VC to block self-fertilization. In this process, the primary binding ability, which is mediated by the interaction between CiVC57 and CiUrabin, may be weakened by unknown mechanisms in response to the self-signal, allowing the occasional detachment of sperm from the VC (27).

Materials and Methods

Preparation of Glycerinated Eggs, VCs, and Sperm. Adult *C. intestinalis* was collected in Onagawa Bay, Japan. Eggs were surgically obtained from the gonoduct. Follicle cells surrounding the egg were removed by shaking in ASW containing 462.01 mM NaCl, 9.39 mM KCl, 10.81 mM $CaCl_2$, 48.27 mM $MgCl_2$, and 10 mM Hepes (pH 8.2). In each experiment, we also used Ca^{2+}-free ASW containing 462.01 mM NaCl, 9.39 mM KCl, 59.08 mM $MgCl_2$, and 10 mM Hepes (pH 8.2). Eggs were treated with 5, 10, 20, and 40% (vol/vol) glycerol-containing ASW for 30 min each. The eggs in 40% glycerol in ASW were washed with ASW and used as glycerinated eggs. The VC was isolated as described below. The eggs were gently homogenized in 0.2× Ca^{2+}/Mg^{2+}-free ASW containing a protease inhibitor mixture [1 mM phenylmethyl sulfonyl fluoride, 10 μg/mL leupeptin, and Complete Mini (Roche)] with a Teflon homogenizer. The homogenate was filtered through a nylon mesh (40 μm), and the VCs remaining on the mesh were extensively washed with ASW by pipetting. Sperm were obtained from spermaducts and stored on ice.

Analysis of the Movement of Glycerinated Eggs in the Self-Insemination and Nonself-Insemination. Sperm were diluted 2,000 times with ASW and added into the suspension of self- and nonself-glycerinated eggs. The sperm behavior of glycerinated eggs was recorded under a microscope. Moving distances of glycerinated eggs were calculated using Bohboh software (Bohboh Soft, Tokyo, Japan) from overlapped images during 1 s at 1 and 5 min after insemination (Fig. 1*A*).

Analysis of Sperm Motility and Flagellar Waveforms. The VCs isolated from self- and nonself-eggs were placed in a one-side-open chamber between a slide glass and a cover glass, the surface of which had been previously coated with 1% BSA to avoid sperm adhesion. Sperm were diluted 2,000-fold with ASW containing 1 mM theophylline (Sigma). The suspension of activated sperm was immediately placed into a chamber containing the VC or the glycerinated egg. Sperm motility and flagellar waveform were observed by a phase-contrast microscope equipped with the power LED stroboscopic illumination system (7) and recorded at 5-ms intervals with a high-speed CCD camera (HAS-220; Ditect). Flagellar curvature was measured as maximal curvature of the principal bend (P-bend) and reverse bend (R-bend) using Bohboh software (7). The bend of larger curvature was defined as P-bend and the other as R-bend according to the definition by Gibbons and Gibbons (28). Flagellar asymmetry was determined from the ratio of maximal P-bend to R-bend. We regarded a maximal value of R-bend under 0.1 as "quiescent." We also defined the value of asymmetry under 1.5 as "normal" and over 1.5 as "largely bending" (Fig. 2*D*).

$[Ca^{2+}]_i$ Fluorescence Imaging of Sperm. Fluorescence attributable to $[Ca^{2+}]_i$ was monitored as described previously (7). Briefly, sperm were suspended in five volumes of low-Ca^{2+} ASW (pH 7.2), containing 460 mM NaCl, 10 mM KCl, 1 mM $CaCl_2$, 36 mM $MgCl_2$, 17.5 mM $MgSO_4$, 0.1 mM EDTA, and 10 mM Hepes-NaOH (pH 7.2), containing 0.05% Cremophor EL (Nacalai Tesque) and 20 μM Fluo-8H-AM (Molecular Probes), and were then incubated for 2 h at 18 °C. The VC was placed between a slide glass and a cover glass, which were coated with 1% BSA. To induce activation of sperm, dye-loaded sperm were diluted 1,000-fold with ASW containing 100 nM SAAF, which was synthesized as described previously (20, 21). Fluorescence signals were recorded with a digital CCD camera (ImagEM, C9100-13; Hamamatsu Photonics) at 20-ms intervals before and after insemination. The intensity of the fluorescence signals was analyzed by Aquacosmos (Hamamatsu Photonics).

ACKNOWLEDGMENTS. We thank the director and staff of Onagawa Field Science Center of Tohoku University, where part of this work was carried out. We also thank the National Bio-Resource Project for providing the ascidian *C. intestinalis*. This study was supported, in part, by a research fellowship of the Japan Society for the Promotion of Science for Young Scientists, the Japanese Association for Marine Biology, and a grant-in-aid for scientific research on innovative areas from the Ministry of Education, Culture, Sports, Science and Technology of Japan.

1. Takayama S, Isogai A (2005) Self-incompatibility in plants. *Annu Rev Plant Biol* 56: 467–489.
2. Morgan TH (1910) Cross- and self-fertilization in *Ciona intestinalis*. *Wilhelm Roux Arch Entwickl Mech Org* 30:206–235.
3. Rosati F, de Santis R (1978) Studies on fertilization in the Ascidans. I. Self-sterility and specific recognition between gametes of *Ciona intestinalis*. *Exp Cell Res* 112:111–119.
4. Kawamura K, Fujita H, Nakauchi M (1987) Cytological characterization of self incompatibility in gametes of the ascidian, *Ciona intestinalis*. *Dev Growth Differ* 29: 627–642.
5. Harada Y, et al. (2008) Mechanism of self-sterility in a hermaphroditic chordate. *Science* 320:548–550.
6. Yamada L, Saito T, Taniguchi H, Sawada H, Harada Y (2009) Comprehensive egg coat proteome of the ascidian *Ciona intestinalis* reveals gamete recognition molecules involved in self-sterility. *J Biol Chem* 284:9402–9410.
7. Shiba K, Baba SA, Inoue T, Yoshida M (2008) Ca^{2+} bursts occur around a local minimal concentration of attractant and trigger sperm chemotactic response. *Proc Natl Acad Sci USA* 105:19312–19317.
8. Lambert CC, Lambert G (1981) The ascidian sperm reaction: Ca^{2+} uptake in relation to H^+ efflux. *Dev Biol* 88:312–317.
9. Lambert CC, Koch RA (1988) Sperm binding and penetration during ascidian fertilization. *Dev Growth Differ* 30:325–336.
10. Okamura Y, et al. (2005) Comprehensive analysis of the ascidian genome reveals novel insights into the molecular evolution of ion channel genes. *Physiol Genomics* 22:269–282.
11. Hanaoka K, et al. (2000) Co-assembly of polycystin-1 and -2 produces unique cation-permeable currents. *Nature* 408:990–994.
12. Kierszenbaum AL (2004) Polycystins: What polycystic kidney disease tells us about sperm. *Mol Reprod Dev* 67:385–388.
13. Delmas P, et al. (2004) Gating of the polycystin ion channel signaling complex in neurons and kidney cells. *FASEB J* 18:740–742.
14. Butscheid Y, et al. (2006) Polycystic kidney disease and receptor for egg jelly is a plasma membrane protein of mouse sperm head. *Mol Reprod Dev* 73:350–360.
15. Neill AT, Moy GW, Vacquier VD (2004) Polycystin-2 associates with the polycystin-1 homolog, suREJ3, and localizes to the acrosomal region of sea urchin spermatozoa. *Mol Reprod Dev* 67:472–477.
16. Yoshida M, Inaba K, Ishida K, Morisawa M (1994) Calcium and cyclic AMP mediate sperm activation, but Ca^{2+} alone contributes sperm chemotaxis in the ascidian, *Ciona savignyi*. *Dev Growth Differ* 36:589–595.
17. Brokaw CJ (1979) Calcium-induced asymmetrical beating of triton-demembranated sea urchin sperm flagella. *J Cell Biol* 82:401–411.
18. Gibbons BH, Gibbons IR (1980) Calcium-induced quiescence in reactivated sea urchin sperm. *J Cell Biol* 84:13–27.
19. Yoshida M, Murata M, Inaba K, Morisawa M (2002) A chemoattractant for ascidian spermatozoa is a sulfated steroid. *Proc Natl Acad Sci USA* 99:14831–14836.
20. Oishi T, Tsuchikawa H, Murata M, Yoshida M, Morisawa M (2003) Synthesis of endogenous sperm-activating and attracting factor isolated from ascidian *Ciona intestinalis*. *Tetrahedron Lett* 44:6387–6389.
21. Oishi T, Tsuchikawa H, Murata M, Yoshida M, Morisawa M (2004) Synthesis and identification of an endogenous sperm activating and attracting factor isolated from eggs of the ascidian *Ciona intestinalis*; an example of nanomolar-level structure elucidation of novel natural compound. *Tetrahedron* 60:6971–6980.
22. Thomas SG, Franklin-Tong VE (2004) Self-incompatibility triggers programmed cell death in Papaver pollen. *Nature* 429:305–309.
23. Iwano M, Takayama S (2012) Self/non-self discrimination in angiosperm self-incompatibility. *Curr Opin Plant Biol* 15:78–83.
24. Rea AC, Nasrallah JB (2008) Self-incompatibility systems: Barriers to self-fertilization in flowering plants. *Int J Dev Biol* 52:627–636.
25. Iwano M, et al. (2004) Ca^{2+} dynamics in a pollen grain and papilla cell during pollination of Arabidopsis. *Plant Physiol* 136:3562–3571.
26. Harada Y, Sawada H (2008) Allorecognition mechanisms during ascidian fertilization. *Int J Dev Biol* 52:637–645.
27. Yamaguchi A, et al. (2011) Identification and localization of the sperm CRISP family protein CiUrabin involved in gamete interaction in the ascidian *Ciona intestinalis*. *Mol Reprod Dev* 78:488–497.
28. Gibbons BH, Gibbons IR (1972) Flagellar movement and adenosine triphosphatase activity in sea urchin sperm extracted with triton X-100. *J Cell Biol* 54:75–97.